Sertoli Cell Processes Have Axoplasmic Features: An Ordered Microtubule Distribution and an Abundant High Molecular Weight Microtubule-associated Protein (Cytoplasmic Dynein)

M. Diana Neely and Kim Boekelheide

Department of Pathology and Laboratory Medicine, Brown University, Providence, Rhode Island

Abstract. Microtubules in the cytoplasm of rat Sertoli cell stage VI–VIII testicular seminiferous epithelium were studied morphometrically by electron microscopy. The Sertoli cell microtubules demonstrated axonal features, being largely parallel in orientation and predominantly spaced one to two microtubule diameters apart, suggesting the presence of microtubule-bound spacer molecules. Testis microtubule-associated proteins (MAPs) were isolated by a taxol, salt elution procedure. Testis MAPs promoted microtubule assembly, but to a lesser degree than brain MAPs. High molecular weight MAPs, similar in electrophoretic mobilities to brain MAP-1 and MAP-2, were prominent components of total testis MAPs, though no shared immunoreactivity was detected between testis and brain high molecular weight MAPs using both polyclonal and monoclonal antibodies. Unlike brain high molecular weight MAPs, testis high molecular weight MAPs were not heat stable. Testis MAP composition, studied on postnatal days 5, 10, 15, and 24 and in the adult, changed dramatically during ontogeny. However, the expression of the major testis high molecular weight MAP, called HMW-2, was constitutive and independent of the development of mature germ cells. The Sertoli cell origin of HMW-2 was confirmed by identifying this protein as the major MAP found in an enriched Sertoli cell preparation and in two rat models of testicular injury characterized by germ cell depletion. HMW-2 was selectively released from testis microtubules by ATP and co-purified by sucrose density gradient centrifugation with MAP-1C, a neuronal cytoplasmic dynein. The inhibition of the microtubule-activated ATPase activity of HMW-2 by vanadate and *erythro*-(2-hydroxy-3-nonyl)adenine and its proteolytic breakdown by vanadate-dependent UV photocleavage confirmed the dynein-like nature of HMW-2. As demonstrated by this study, the neuronal and Sertoli cell cytoskeletons share morphological, structural and functional properties.

THE neuron is a very asymmetrical cell with multiple long processes, the dendrites and the axon. A striking feature of the neuronal cytoskeleton is its highly regular organization. The microtubules in dendrites and nonmyelinated axons are uniformly distributed, parallel to each other and to the axis of the cell process, and equidistantly spaced apart (Wuerker and Kirkpatrick, 1972). High molecular weight microtubule-associated proteins (MAPs)[1] are likely responsible for this regular microtubule arrangement in neuronal processes (Hirokawa et al., 1985; Vallee and Bloom, 1984).

Two high molecular weight MAPs, called MAP-1 and MAP-2, are major components of isolated neuronal microtubules (Olmsted, 1986; Sloboda et al., 1975) and are associated with neuronal microtubules in situ (Hirokawa et al., 1985; Izant and Mcintosh, 1980). Further analysis of these neuronal high molecular weight MAPs has indicated the presence of multiple MAP-1 and MAP-2 proteins (Bloom et al., 1984; Kim et al., 1979). Of particular interest is MAP-1C, now identified as a cytoplasmic dynein (Paschal et al., 1987) which may be responsible for retrograde organelle transport in the axoplasm (Paschal and Vallee, 1987).

The Sertoli cell, the supportive cell of the testicular seminiferous epithelium, is also a highly asymmetrical cell. The Sertoli cell is columnar in form with multiple processes that radiate from a basal trunk toward the lumen of the seminiferous tubule to partly or completely surround the developing germ cells (Fawcett, 1975; Russell et al., 1983; Weber et al., 1983; Wong and Russell, 1983). Qualitatively, the morphological arrangement of microtubules in the apical Sertoli cell cytoplasm is reminiscent of that in the axoplasm (Fawcett, 1975; Vogl et al., 1983*a*,*b*).

Although immunological approaches have demonstrated cross reactivity of antibodies against MAP-1 and MAP-2 in nonneuronal tissues (Valdivia et al., 1982; Wiche et al., 1984), quantitative comparisons of MAP-1 and MAP-2 mRNA

1. *Abbreviation used in this paper*: MAP, microtubule-associated protein.

levels (Lewis et al., 1986*a*,*b*) and of microtubule protein composition (Parysek et al., 1984*a*) have shown that expression of brain high molecular weight MAPs in nonneuronal tissues is absent or exceedingly low. A crude preparation of testis microtubules suggested that high molecular weight MAPs may be abundant in this tissue (Wiche et al., 1984). In a preliminary report from our laboratory, high molecular weight MAPs, at least one of which is localized in Sertoli cells, were described as major components of testis microtubules.

In this study, we describe a nonneuronal cell type, the testicular Sertoli cell, in which there is a regular microtubule organization accompanied by the presence of an abundant high molecular weight MAP. An isolation procedure for testis MAPs is presented along with a description of their assembly-promoting properties, heat stability, and appearance during ontogeny in the rat. Finally, we characterize the major Sertoli cell high molecular weight MAP as a cytoplasmic dynein similar in structure to neuronal MAP-1C.

Materials and Methods

General

Unless otherwise indicated, all chemicals and reagents were obtained from Sigma Chemical Co. (St. Louis, MO). Protein concentrations were determined by the method of Lowry et al. (1951). SDS-PAGE was performed according to Laemmli (1970) with staining by Coomassie Brilliant Blue R or the silver technique as described by Merril et al. (1981). Molecular mass standards included rabbit muscle myosin (205 kD), *Escherichia coli* β-galactosidase (116 kD), rabbit muscle phosphorylase B (97.4 kD), BSA (66 kD), and ovalbumin (45 kD). Electrophoretic transfer to nitrocellulose was performed as described by Gibson (1981) using chymotrypsin (50 μg/ml) to facilitate transfer. Primary antibodies tested were: a polyclonal antibody to bovine brain heat-stable MAPs (Miles Scientific, Naperville, IL), monoclonal antibodies to MAP-1A and MAP-2 (the generous gift of Dr. R. B. Vallee; Vallee and Luca, 1985), and a second monoclonal antibody to MAP-2 (the generous gift of Dr. K. S. Kosik; Kosik et al., 1984). Reactivity was detected using as the secondary antibody either biotinylated anti-rabbit IgG or anti-mouse IgG (Vector Laboratories, Burlingame, CA) followed by peroxidase-coupled avidin (Vectastain ABC Kit) and 3,3′-diaminobenzidine or affinity-purified peroxidase-coupled anti-rabbit IgG or anti-mouse IgG (Cappell Laboratories, Malvern, PA) followed by 3,3′-diaminobenzidine. Nonspecific binding was blocked with either 5% BSA or 0.1% gelatin (Bio-Rad, Rockville Center, NY). Testis MAPs were tested for heat stability following the procedure of Vallee (1985).

Sertoli Cell Morphometry

Charles River CD rats (200 g) were anesthetized with pentobarbital, injected with heparin into the inferior vena cava, and then perfused through the ascending aorta with a vasodilator solution (0.01% sodium nitroprusside and 0.1% procaine in Ringer's salt solution without calcium chloride) followed by a modified Karnovsky's fixative (2.5% glutaraldehyde, 2% formaldehyde, and 1% tannic acid in 0.1 M cacodylate, pH 7.2). Tissue fragments were post-fixed in osmium tetroxide, dehydrated, and embedded in Spurr's medium (Electron Microscopy Sciences, Fort Washington, PA). Semi-thin sections were scanned for cross sections of stage VI-VIII seminiferous tubules. Thin sectioning yielded consistently gold-colored sections (~90 nm in thickness). The sections were stained with lead citrate and uranyl acetate and examined in a Philips 410 transmission electron microscope. A morphometric analysis was performed on the microtubules present in the columns of Sertoli cell cytoplasm in the middle portion of the seminiferous epithelium, at the level of the spermatocyte and basal round spermatid layers. Negatives of 28,800× were examined with a 6× magnifier fitted with a reticle scaled to .005 in (4.4 nm). The microtubules had an average diameter of 22 nm. For each microtubule, two measurements were obtained: (*a*) the relative angle of the microtubule, and (*b*) the distance from that microtubule to the nearest neighboring microtubule. The relative angle of a microtubule was defined as the absolute value of its angular deviation from the mean parallel direction of all microtubules measured on a given negative. The distance to the nearest neighboring microtubule was defined as the closest intermicrotubule distance observed regardless of direction.

Germ Cell–depleted Rat Models

Charles River CD rats (n = 6, mean body weight of 305 g) were rendered cryptorchid by translocating the testes from the scrotum to the abdominal cavity and suturing the gubernaculum testis to the anterior abdominal wall. Atrophic testes (mean testis weight of 0.74 g) were obtained 16 wk after surgery. Charles River CD rats (n = 8, mean body weight 185 g) were treated for 5 wk with 1% 2,5-hexanedione in the drinking water at an average dose rate of 7.1 mM/kg per d (Boekelheide, 1988*a*). Atrophic testes (mean testis weight of 0.69 g) were obtained after a 16-wk recovery period. The normal adult rat testis weight is ~1.7 g (Boekelheide, 1988*a*). In both of these rat models, the testicular content of mature germ cells which contain axonemal structures is markedly reduced or eliminated (Boekelheide, 1988*a*; Nelson, 1951).

Preparation of Isolated Sertoli Cells

Sertoli cells were isolated from 18–20-d-old rats (Chapin et al., 1987; some preparations were kindly provided by Dr. Robert E. Chapin, NIEHS [Research Triangle Park, NC]) and processed without culturing. The preparation of "isolated Sertoli cells" was composed of ~45% germ cells (spermatogonia and spermatocytes) and 55% nongerm cells, as determined by nuclear morphology after cytospin centrifugation and staining with hematoxylin and eosin. The nongerm cells were predominantly Sertoli cells with few Leydig cells (<2% of cells stained for the Leydig cell-specific enzyme activity 3-β-OH-steroid dehydrogenase; Chapin, personal communication) and less than 4% peritubular cells (Chapin et al., 1987). Crude homogenates were prepared by suspension of the isolated cells in 1 vol of extraction buffer (100 mM 2[N-morpholino]ethane sulfonic acid [MES], 1 mM EGTA, 0.5 mM $MgCl_2$, 4 M glycerol, pH 6.75) followed by sonication.

Isolation of MAPs

MAPs were isolated from Sertoli cell preparations, testes and brains of Charles River CD rats by using taxol (kindly provided by Dr. Mathew Suffness, Chief, Natural Products Branch, National Cancer Institute, Bethesda, MD) to induce microtubule polymerization (Vallee, 1982). Brains were processed by three strokes of a glass/Teflon homogenizer at 1,100 rpm in 1 vol of extraction buffer. Testes were decapsulated and similarly homogenized in 1 vol of extraction buffer with 0.2 mM phenylmethylsulfonyl fluoride (PMSF), 0.1 mg/ml soybean trypsin inhibitor, and 2 μg/ml leupeptin. The crude homogenates were centrifuged at 100,000 *g* for 30 min at 4°C. The supernatants were again centrifuged at 130,000 *g* for 45 min at 4°C. Taxol (20 μM) and GTP (1 mM) were added to the resulting high speed supernatants and microtubule polymerization was allowed to proceed at 37°C for 5 min followed by 25 min on ice. The microtubules were sedimented at 100,000 *g* for 30 min at 4°C through a 25% sucrose cushion. The pellets were resuspended in assembly buffer (100 mM MES, 1 mM EGTA, 1 mM $MgCl_2$, pH 6.75) containing 20 μM taxol and 1 mM GTP in 10% of the original high speed supernatant volume. The samples were left on ice for 5 min and then centrifuged at 75,000 *g* for 30 min at 4°C. The resulting microtubule pellets were resuspended and gently homogenized in 7% of the original high speed supernatant volume in assembly buffer with 20 μM taxol, 1 mM GTP, and 0.75 or 0.5 M NaCl at 37°C. After 5 min at 37°C, the samples were centrifuged at 75,000 *g* for 30 min at 29°C. The MAPs were recovered in the supernatants. The addition of glycerol to the extraction buffer, a departure from the reference procedure (Vallee, 1982), approximately doubled the yield of microtubules and MAPs from the testis. The average yield of testis MAPs was 0.15 mg/ml high speed supernatant.

Microtubule Asssembly

Brain or testis MAPs, desalted by passage over a G-25 Sephadex gel filtration column (Pharmacia Fine Chemicals, Piscataway, NJ), were added at various concentrations to bovine brain tubulin (Boekelheide, 1987) present at a final concentration of 2 mg/ml in assembly buffer. Microtubule assembly was monitored spectrophotometrically at 37°C upon addition of 0.25 mM GTP (Boekelheide, 1987). After a 30-min polymerization, microtubule aliquots were negatively stained with 1% uranyl acetate and viewed in a Philips 410 transmission electron microscope. Microtubule depolymerization was induced by circulating ice-cold water through the cuvette holder housing of the spectrophotometer.

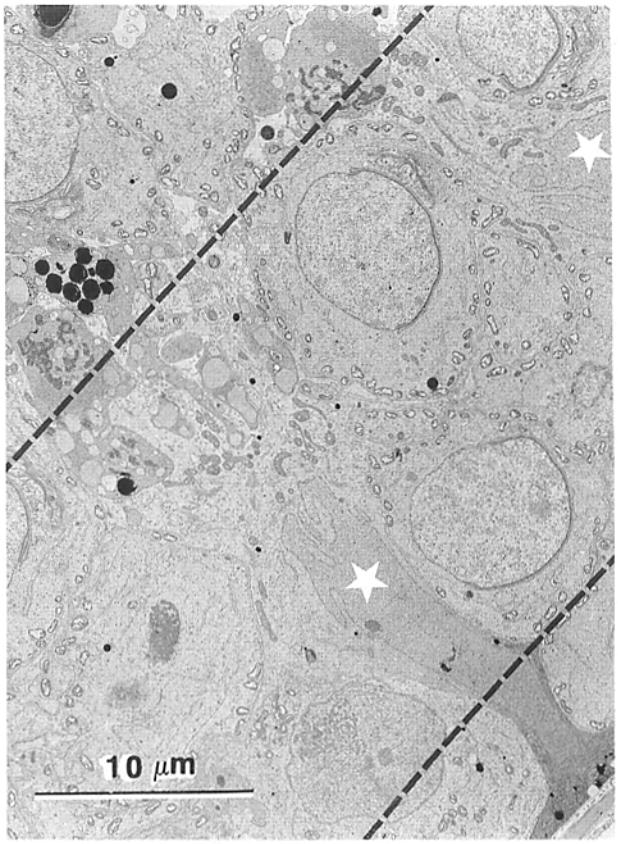

Figure 1. This stage VIII seminiferous tubule contains two Sertoli cell nuclei (☆) with abundant apical cytoplasm surrounding developing germ cells. The middle portion of the seminiferous epithelium (between dotted lines) was examined morphometrically.

Figure 2. Two stage VII spermatids (*N*, spermatid nuclei; *A*, spermatid acrosome) surround a column of Sertoli cell cytoplasm. The Sertoli cell cytoplasm contains abundant microtubules (*arrowheads*) which are packed in a highly ordered, parallel arrangement.

Characterization of Cytoplasmic Dynein

Cytoplasmic dynein was isolated from bovine brain white matter and from rat testis as described by Paschal et al. (1987) with some modifications. Taxol (20 μM) was added to high speed supernatants prepared from tissue homogenates (as described above) and microtubules were polymerized for 15 min at 37°C followed by 15 min on ice. The microtubules were centrifuged at 100,000 *g* through a 25% sucrose cushion for 30 min at 4°C. The pellets were resuspended in assembly buffer containing 20 μM taxol in 10% of the original high speed supernatant volume. The samples were left on ice for 5 min and then centrifuged at 75,000 *g* for 30 min at 4°C. The microtubule pellets were resuspended in the same volume of assembly buffer with 20 μM taxol, 5 mM $MgCl_2$, and 5 mM GTP and incubated at room temperature for 10 min and then 5 min at 37°C, followed by centrifugation at 75,000 *g* for 30 min at 29°C. The GTP extraction procedure was repeated with 1 mM $MgCl_2$ and 1 mM GTP. Finally, the microtubules were suspended in 5% of the original high speed supernatant volume of assembly buffer containing 20 μM taxol, 10 mM $MgCl_2$, and 10 mM ATP and extracted as above. The average yield of ATP eluate protein was 26 μg (six isolations) and 17 μg (two isolations) per ml of the original high speed supernatant from the testis and bovine brain white matter, respectively.

Further purification of cytoplasmic dynein, achieved by sucrose density gradient centrifugation using the Tris-HCl buffer system (Paschal et al., 1987), was performed before conducting ATPase assays (Paschal et al., 1987) and vanadate photocleavage (King and Witman, 1987).

Results

Microtubule Organization in the Sertoli Cell

Since the Sertoli cell cytoskeleton undergoes a stage-dependent cyclic reorganization (Amlani and Vogl, 1988), the ultrastructural examination of the Sertoli cell cytoplasm was confined to a few specific stages and a specific depth of the seminiferous epithelium. Only the columns of Sertoli cell cytoplasm spanning the spermatocyte and basal round spermatid layers in stage VI–VIII seminifierous epithelium (as defined by Leblond and Clermont, 1952) were studied (Fig. 1). By electron microscopy, these Sertoli cell columns were readily distinguished as bands of cytoplasm rich in mitochondria, vesicles, and cytoskeletal elements. At high magnification, abundant microtubules were observed in a qualitatively highly ordered arrangement (Fig. 2).

A morphometric analysis of Sertoli cell intermicrotubule distances and angular deviations was performed. A total of 851 microtubules (range 160–493 microtubules per rat) were counted in three rats. The microtubules were highly parallel in orientation (Fig. 3). In addition, the microtubules tended to maintain a consistent intermicrotubule distance (Fig. 4). The unweighted median closest intermicrotubule distance was 35.3 ± 10.2 nm ($n = 3$).

Isolation of Testis MAPs and Comparison with Brain MAPs

Microtubules were purified from testis homogenates by a

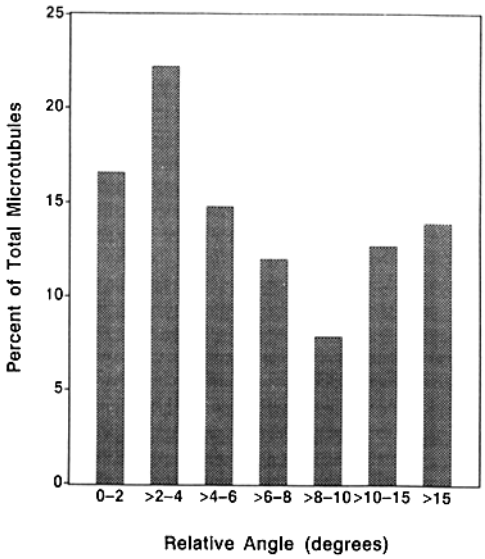

Figure 3. The unweighted average percent of total microtubules with the depicted relative angle was determined in columns of rat stage VI–VIII Sertoli cell cytoplasm (n = 3). The relative angle of a microtubule was defined as the absolute value of its angular deviation from the mean parallel direction of all microtubules measured on a given electron microscopic negative.

modification of the taxol, salt-extraction method reported by Vallee (1982). With taxol-induced polymerization, a wide variety of proteins co-purified with tubulin (Fig. 5, lane *3*). A group of high molecular weight proteins, a major component of these co-purifying proteins, was specifically associated with microtubules since they were not released during washing of the microtubule pellet (Fig. 5, lane *5*). The MAP preparations used in subsequent studies were obtained by a NaCl wash (Fig. 5, lane *6*). When colchicine was present during the isolation procedure, no microtubules or MAPs were isolated (data not shown).

Testis MAPs were salt eluted from taxol-polymerized

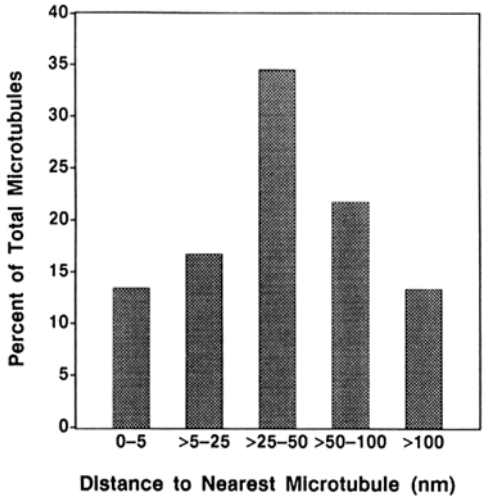

Figure 4. The unweighted average percent of total microtubules with the depicted distance to the nearest adjacent microtubule was determined in columns of rat stage VI–VIII Sertoli cell cytoplasm (n = 3).

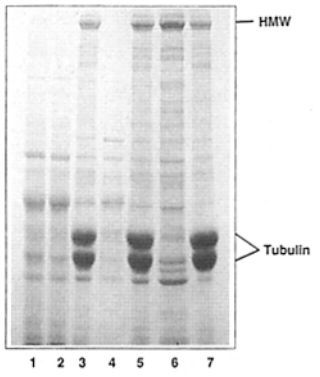

Figure 5. Isolation procedure for testis MAPs (SDS-PAGE, 7% gel, Coomassie Blue-stained). Microtubules were polymerized from a high speed testis supernatant (lane *1*) by addition of taxol and GTP. Centrifugation gave a microtubule-depleted supernatant (lane *2*) and a microtubule pellet (lane *3*). After washing and re-centrifugation (lane *4*, supernatant; lane *5*, washed microtubule pellet), the microtubules were re-suspended in assembly buffer with taxol, GTP and NaCl. A final centrifugation left the MAPs in the supernatant (lane *6*) and microtubules in the pellet (lane *7*). The locations of tubulin and high molecular weight MAPs (*HMW*) are indicated.

microtubules and compared to brain MAPs prepared in an identical manner. Three high molecular weight MAPs, labeled HMW-1, HMW-2, and HMW-3, were clearly identified in all testis MAP preparations (Fig. 6). A fourth minor protein component, exhibiting a slower electrophoretic mobility than the three major high molecular weight MAPs, was inconsistently isolated with testis microtubules. HMW-1 exhibited a slower electrophoretic mobility than brain MAP-1. HMW-2 and HMW-3, the major testis high molecular weight MAPs in all preparations, showed electrophoretic mobilities slower (HMW-2) and faster (HMW-3) than brain MAP-2. Besides the high molecular weight MAPs, numerous additional proteins were isolated from both brain and testis.

Microtubule Assembly and Immunoreactivity of Testis MAPs

Brain MAPs characteristically promote microtubule assembly in buffer systems wherein pure tubulin alone will not assemble (Murphy and Borisy, 1975; Sloboda et al., 1976). Testis MAPs also demonstrated this capacity to enhance microtubule assembly (Fig. 7). Initial rate and the total amount of microtubule assembly increased in a concentration-dependent fashion. The degree of microtubule assembly enhancement by testis MAPs was less than that achieved with brain MAPs (Fig. 7, compare lines *D* and *F*). Mixtures of

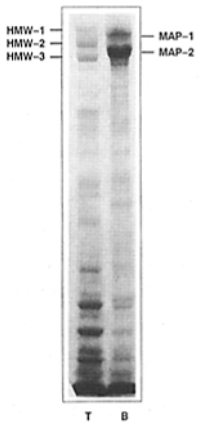

Figure 6. Comparison of testis MAPs (lane *T*) and brain MAPs (lane *B*) by SDS-PAGE on a 5% Coomassie Blue-stained gel. The positions of brain MAP-1 and brain MAP-2 are indicated along with the three prominent high molecular weight testis MAPs called HMW-1, HMW-2, and HMW-3.

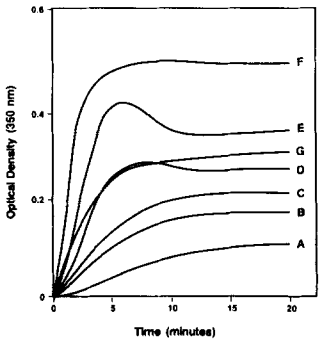

Figure 7. Testis MAPs promote microtubule polymerization. MAPs were added to bovine brain tubulin (2 mg/ml) in assembly buffer. Microtubule polymerization was induced upon addition of GTP and warming to 37°C. Assembly was monitored by measuring the optical density at 350 nm. Testis MAPs concentration: (*A*) 0.65 mg/ml, (*B*) 0.85 mg/ml, (*C*) 1.3 mg/ml, (*D*) 1.7 mg/ml, (*E*) 2.6 mg/ml. Brain MAPs concentration: (*F*) 1.5 mg/ml. Curve (*G*) was generated by the combination of 0.9 mg/ml testis MAPs plus 0.4 mg/ml brain MAPs.

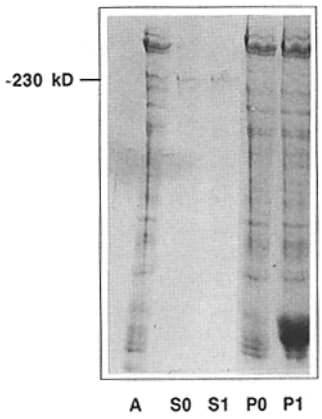

Figure 8. The heat stability of testis MAPs was analyzed by SDS-PAGE on a 6% gel stained with Coomassie Blue. Testis MAPs (0.9 mg/ml) with or without bovine brain tubulin (lanes *S0* and *P0*: no tubulin; lanes *S1* and *P1*: 0.4 mg/ml tubulin) were boiled in assembly buffer with 0.75 M NaCl and 10 mM DTT for 5 min and then centrifuged. The supernatants (lanes *S0* and *S1*) and pellets (lanes *P0* and *P1*) are compared with untreated testis MAPs (lane *A*).

testis MAPs and brain MAPs had an additive effect in promoting microtubule assembly (Fig. 7, compare lines *B*, *C*, and *G*). Microtubules formed with testis MAPs had the usual ultrastructural appearance when visualized by negative stain and were cold sensitive (data not shown).

Brain and testis MAPs were also compared for immunologic similarities. All antibodies tested, including a polyclonal antibody developed against brain heat-stable MAPs and monoclonal antibodies against brain MAP-1A and MAP-2, showed no reactivity with testis MAPs (data not shown).

Heat Stability of Total Testis MAPs

All major brain high molecular weight MAPs remain soluble after boiling for 5 min in 0.75 M NaCl with 10 mM DTT (Vallee, 1985). In the presence of tubulin, brain MAP-2 selectively remains soluble while MAP-1 precipitates (Vallee, 1985). The high molecular weight testis MAPs precipitated on boiling in both the presence and absence of added bovine brain tubulin (Fig. 8). Addition of greater amounts of bovine brain tubulin (up to 1.2 mg/ml) or testis microtubules (1 mg/ml) did not alter the heat sensitivity of testis MAPs. A minor group of proteins with molecular masses of ~230 kD remained soluble after boiling (Fig. 8).

Cellular Origin of High Molecular Weight MAPs

The testis is composed of several different cell types. The somatic cells unique to the testis include the Leydig cells, Sertoli cells and peritubular cells. These somatic cells are constitutively present while the germ cells, beginning with a small number of primitive spermatogonial precursors, expand in number and mature in a well-defined time sequence during postnatal development of the rat testis (Clermont and Perey, 1957). Between postnatal days 4 and 9 spermatogonial mitoses take place, by day 15 spermatocyte meiosis begins, and by day 25 the first spermatids appear. The axonemal structures appear after day 25 during spermatid maturation. Given this controlled sequence of development, the appearance of specific MAPs at certain times during ontogeny could provide information about the cell type of origin of these proteins.

Testis MAPs isolated from adult rats and rats of 5 (data not shown), 10, 15, and 24 d of age demonstrated marked differences in protein concentration and composition (Fig. 9). The young rats all had a prominent doublet of MAP proteins of molecular weight 180,000 which peaked in concentration at 15 d. Of the high molecular weight MAPs, HMW-3 was absent from the youngest rats and appeared as only a minor band in rats 24 d old (Fig. 9, lane *24*). HMW-1 and HMW-2 were present at all ages, suggesting their origin from Sertoli, Leydig, or peritubular cells.

To further establish the somatic cell origin of these high molecular weight MAPs, microtubules were purified from germ cell-depleted rat testes. The normal adult rat testis contains many more germ cells than somatic cells (a germ cell to Sertoli cell ratio of greater than 27:1; Clermont and Morgentaler, 1955). We therefore used two experimental models, cryptorchidism and 2,5-hexanedione intoxication, known to enhance the relative somatic cell content of the testes. In experimental cryptorchidism, the testes are translocated from the scrotal sac and held in the abdominal cavity by sutures. The elevated temperature of the abdominal cavity relative to the scrotum results in a profound loss of germ cells (Nelson, 1951). Intoxication with 1% 2,5-hexanedione in the drinking water for 5 wk markedly reduces the germ cell content of the rat testis with the majority of animals demonstrating a germ cell to Sertoli cell ratio of less than 1:50 (Boekelheide, 1988*a*). Both HMW-1 and HMW-2 were prominent MAP

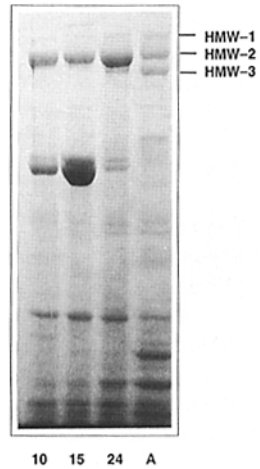

Figure 9. Testis MAPs were prepared from rats of various ages (lane *10*, 10-d-old; lane *15*, 15-d-old; lane *24*, 24-d-old; lane *A*, adult) and analyzed by SDS-PAGE on a 5% gel stained with Coomassie Blue.

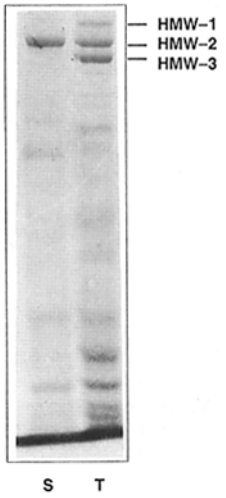

Figure 10. Sertoli cell MAPs (lane *S*) and total testis MAPs (lane *T*) were compared by SDS–PAGE on a 5% gel stained with Coomassie Blue.

components in these germ cell depleted preparations supporting their origin from somatic cells.

To identify the somatic cell type of origin of these high molecular weight MAPs, microtubules were purified from "isolated Sertoli cells" derived from 18–20-d-old rats and compared with adult rat testis MAPs (Fig. 10). The "isolated Sertoli cells," though contaminated with immature germ cells, contained <2% Leydig cells and <4% peritubular cells. Of the high molecular weight MAPs, only HMW-2 was identified as a major component of this prepubertal Sertoli cell–enriched preparation.

HMW-2 is a Testicular Cytoplasmic Dynein

Incubation of bovine brain white matter microtubules with ATP and $MgCl_2$ specifically releases MAP-1C, a protein complex composed of a high molecular weight protein and associated light chains (Paschal et al., 1987). This protein complex exhibits microtubule-dependent ATPase activity and is sensitive to vanadate-dependent UV photocleavage, properties characteristic of a cytoplasmic dynein (Paschal et al., 1987).

Testis MAPs were examined for the nucleotide-dependence of their binding to microtubules. Incubation of testis microtubules with 1–5 mM GTP or 10 mM 5′-adenylylimidodiphosphate (a nonhydrolyzable ATP analogue) plus equimolar $MgCl_2$ failed to release significant amounts of high molecular weight MAPs (data not shown). On the other hand, incubation with 10 mM $MgCl_2$ and 10 mM ATP resulted in the dissociation of HMW-2 and numerous lower molecular weight proteins from microtubules (Fig. 11, lane *2*). Many of the ATP-released testis MAPs were similar to ATP-released brain MAPs in electrophoretic mobility (Fig. 11, compare lanes *1* and *2*).

ATP extracts of testis and brain microtubules were further purified by sucrose density gradient centrifugation. The HMW-2 and MAP-1C protein complexes eluted in the same fractions of a 5–20% sucrose gradient, thus exhibiting similar sedimentation coefficients. Several of the proteins which co-fractionated in the sucrose gradient with HMW-2 and MAP-1C demonstrated identical electrophoretic mobilities (Fig. 11, compare lanes *3* and *4*). Particularly noteworthy was a 90-kD protein found in both testis and brain preparations (reported as 74 kD by Paschal et al., 1987). A 173-kD

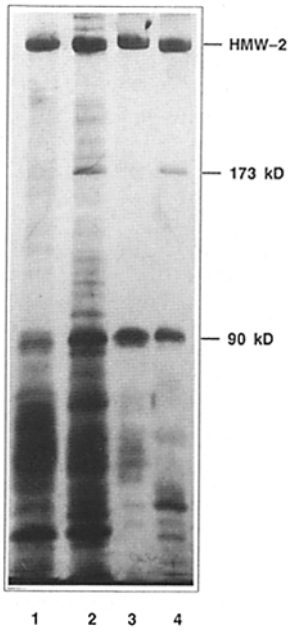

Figure 11. Taxol-induced bovine brain white matter and rat testis microtubules were extracted with 5 mM $MgCl_2$ with 5 mM GTP followed by 1 mM $MgCl_2$ with 1 mM GTP and finally 10 mM $MgCl_2$ with 10 mM ATP. The ATP eluates (lane *1*: brain; lane *2*: testis) and the peak fractions (lane *3*: MAP-1C; lane *4*: HMW-2) of a 5–20% sucrose density gradient centrifugation of these eluates were analyzed by SDS–PAGE on a 6% silver-stained gel.

protein was present as a prominent component in testis-derived material and could be visualized as a very minor component on silver stained gels of brain-derived material. This 173-kD protein was partially released when testis microtubules were extracted with 5 mM GTP and 5 mM $MgCl_2$, 1 mM GTP, and 1 mM $MgCl_2$, or 10 mM 5′-adenylylimidodiphosphate plus 10 mM $MgCl_2$ (data not shown).

Microtubule-activated and microtubule-independent ATPase activity was determined in the sucrose gradient fractions of ATP-released testis MAPs (Fig. 12). A low level of ATPase activity was observed in all fractions with the peak of ATPase activity coinciding with the HMW-2 fractions. The ATPase activity in the HMW-2 fractions was stimulated approximately twofold by the addition of taxol-stabilized microtubules. The specific activity of the microtubule-activated ATPase averaged 171 nmol/min per mg (four isolations) in the peak HMW-2 fractions.

Pharmacological studies were carried out to analyze the properties of the ATPase activity associated with HMW-2. Vanadate, a known inhibitor of dynein ATPases (Gibbons et al., 1978), significantly inhibited the ATPase activity of HMW-2 at micromolar concentrations (Table I). *Erythro*-(2-hydroxy-3-nonyl)adenine, an inhibitor of dynein ATPases (Penningroth et al., 1982) and a specific inhibitor of retrograde axonal transport (Forman et al., 1983), only inhibited the ATPase activity if present in large excess over ATP. The lack of significant inhibition of the HMW-2 ATPase activity by azide, oligomycin, and ouabain demonstrated the absence of mitochondrial and Na+/K+ ATPases in the preparation.

To further establish the dynein-like character of HMW-2, this protein was UV irradiated in the presence of vanadate and ATP. Vanadate-dependent photocleavage of HMW-2 (Fig. 13) gave rise to two high molecular weight fragments of 210,000 and 250,000 which showed the same electrophoretic mobility as the photocleavage fragments derived from MAP-1C (reported as 185,000 and 225,000 by Paschal et al., 1987).

ATPase activities were also determined in ATP eluates of microtubules isolated from the testes of germ cell depleted

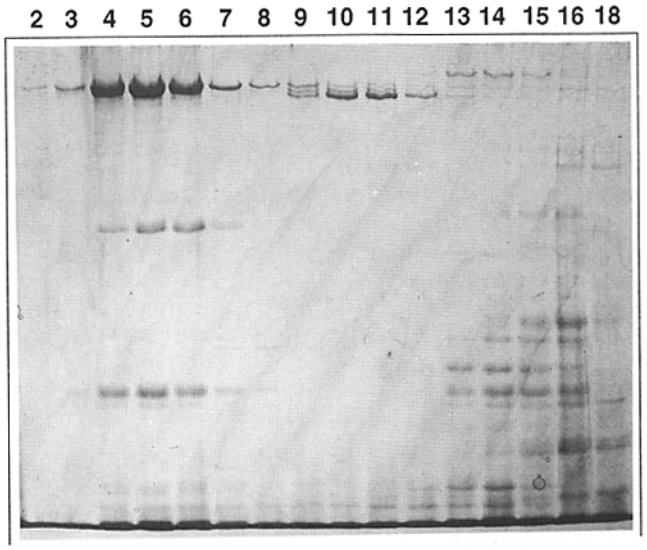

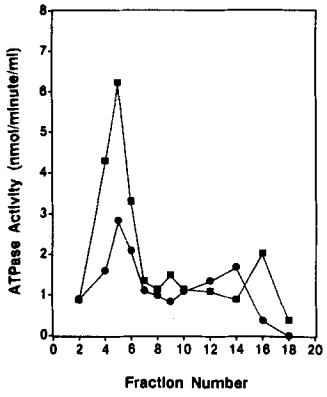

Figure 12. Fractionation of an ATP extract of testis microtubules by a 5–20% sucrose density gradient centrifugation. (*Top*) Sucrose gradient fractions (numbered starting at the bottom of the gradient) were analyzed by SDS-PAGE on a 5% silver-stained gel. (*Bottom*) The ATPase activity in the absence (●) and presence (■) of taxol-stabilized microtubules (4 mg/ml) was determined in the sucrose gradient fractions. The peak ATPase activity co-purified with the peak of HMW-2 (fraction *5*).

Table I. Sensitivity of Testicular HMW-2 ATPase Activity to Various Inhibitors

Inhibitors (concentration)	ATPase activity
	%
None	100
Vanadate (5 μM)	75
Vanadate (50 μM)	58
EHNA (0.4 mM)*	106
EHNA (4 mM)*	7
Azide (1.0 mM)	93
Ouabain (0.1 mM)	97
Oligomycin (25 μM)	95

ATPase activity was determined for testicular HMW-2 after purification by sucrose density gradient centrifugation. HMW-2 was preincubated with the inhibitors for 30 min at room temperature followed by an incubation with 0.4 mM ATP for 30 min at 37°C (Paschal et al., 1987).
* EHNA, *erythro*-(2-hydroxy-3-nonyl)adenine.

rats (treated by experimental cryptorchidism or 2,5-hexanedione intoxication). These ATPase activities were microtubule-stimulated and inhibited by 50 μM vanadate. In addition, ATP eluates of HMW-2 isolated from whole testes, germ cell-depleted testes and Sertoli cell-enriched preparations shared the same vanadate-dependent UV photocleavage pattern, confirming the identity of the protein isolated from Sertoli cells and whole rat testis (data not shown).

Discussion

The morphometric analysis of Sertoli cell microtubules indicated an ordered packing of these cytoskeletal elements within cytoplasmic processes. The Sertoli cell microtubules were largely parallel to one another and were predominantly spaced between one and two microtubule diameters apart. Few microtubules were greater than 100 nm apart. Short intermicrotubule distances can be explained, at least in part, by superimposition within the two-dimensional image of the electron microscopic negative. The overall regular spacing of these microtubules suggested the presence of microtubule-bound spacer molecules.

Taxol-induced microtubule polymerization and salt elution were used to isolate testis MAPs. Total testis MAPs were capable of promoting microtubule polymerization. Three high molecular weight MAPs were observed with the major component called HMW-2. The testis high molecular weight MAPs had electrophoretic mobilities similar to those of brain MAP-1 and MAP-2. However, the testis and brain high molecular weight MAPs shared no immunologic similarities as determined with a polyclonal antibody to brain heat-stable MAPs and monoclonal antibodies to MAP-1A and MAP-2. The testis high molecular weight MAPs were also heat sensitive, distinguishing them from brain MAP-1 and MAP-2 (Vallee, 1985). Indeed, only a minor group of testis MAPs was heat stable; their electrophoretic mobility was consistent with that of the heat stable MAP-4 isoforms known to be present in the testis (Parysek et al., 1984*b*).

HMW-1 was observed at all time points examined during postnatal development while detection of HMW-3 required the presence of maturing germ cells within the testis. HMW-3 was absent in 10- and 15-d-old rat testes, absent in 18-d-old rat Sertoli cells, and present as a minor component in 24-d-old rat testes. During ontogeny in the rat, day 25 represents the

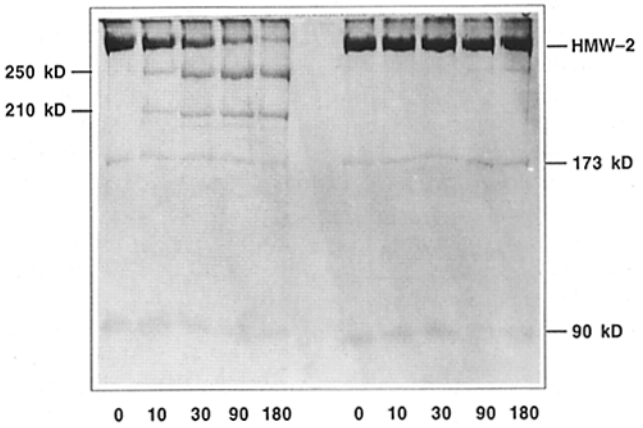

Figure 13. Sucrose density gradient purified HMW-2 was UV irradiated for 0, 10, 30, 90, and 180 min (lanes *0*, *10*, *30*, *90*, and *180*) in the presence of 0.5 mM DTT and 1 mM ATP with 1 mM vanadate (*left*) or without vanadate (*right*). The vanadate-dependent photocleavage products (250 and 210 kD) of HMW-2 are analyzed by SDS-PAGE on a 6% silver-stained gel.

time at which the first spermatids and the first axonemal elements begin to appear in the testis (Clermont and Perey, 1957). Three explanations can be offered concerning the origin of HMW-3: (*a*) this high molecular weight MAP is a protein synthesized by meiotic or post-meiotic germ cells, (*b*) HMW-3 is a Sertoli cell MAP induced by the presence of maturing germ cells, and (*c*) HMW-3 is an acrosome-dependent breakdown product of HMW-2 (the acrosome is a spermatid organelle replete with proteolytic enzymes [Morton, 1976]). Additional structural studies and protein isolations from the various testicular cell types will be required to discriminate among these possibilities.

Three lines of evidence have identified HMW-2 as a Sertoli cell MAP. First, HMW-2 was present by postnatal day 5, the earliest time point examined in a study of the ontogeny of testis MAPs. At this age, the testis is composed predominantly of somatic cells (Sertoli cells, Leydig cells, and peritubular cells) with a few primitive germ cells which contain no axonemal structures. The ratio of germ cells to Sertoli cells within the seminiferous tubules at postnatal day 5 is ~1:24 compared to the adult ratio of greater than 27:1 (Clermont and Morgentaler, 1955; Clermont and Perey, 1957). Second, HMW-2 was the predominant high molecular weight MAP found in the germ cell–depleted testes of rats treated by experimental cryptorchidism or 2,5-hexanedione intoxication. Both of these treatments result in a profound loss of germ cells from the testes and virtual elimination of the mature germ cells (spermatids) which contain axonemal structures (Boekelheide, 1988*a*; Nelson, 1951). The presence of HMW-2 in the testes of the 5-d–old rat as well as in germ cell–depleted testes strongly supports a somatic cell type of origin for this protein. Finally, when MAPs were isolated from an enriched Sertoli cell preparation, which contained few contaminating Leydig cells and peritubular cells, HMW-2 was the predominant protein observed indicating origin from the Sertoli cells.

In examining nucleotide-dependent binding of testis MAPs to testis microtubules, we found that HMW-2 was quantitatively dissociated from microtubules by ATP. HMW-2 showed the same electrophoretic mobility as MAP-1C, a microtubule-associated dynein isolated from brain white matter (Paschal et al., 1987). Both HMW-2 and MAP-1C had multiple co-purifying light chains, several of similar electrophoretic mobility. A prominent protein of 173 kD which co-purified with HMW-2 was observed as only a minor protein in association with MAP-1C. Based upon molecular mass, sedimentation coefficient, and its dissociation from microtubules incubated with 5′-adenylylimidodiphosphate, this 173-kD protein differs from kinesin, another known microtubule-associated ATPase (Brady, 1985; Vale et al., 1986). After purification by sucrose density gradient centrifugation, the specific activity of the HMW-2 ATPase averaged 171 nmol/min per mg, 2 times lower than that of MAP-1C (Paschal et al., 1987). UV irradiation in the presence of vanadate and ATP resulted in the cleavage of HMW-2 into two fragments identical to those produced by the cleavage of MAP-1C.

ATP-dependent release from microtubules, microtubule-stimulated ATPase activity, inhibition of ATPase activity by vanadate and *erythro*-(2-hydroxy-3-nonyl)adenine, vanadate-sensitive photocleavage, and lack of inhibition of ATPase activity by azide, oligomycin and ouabain identify HMW-2 as a dynein. The motility of the dynein-like translocator of bovine brain, MAP-1C, was also inhibited by vanadate and *erythro*-(2-hydroxy-3-nonyl)adenine, but not by azide or ouabain (Paschal and Vallee, 1987). The ATPase activity of two nonmammalian cytoplasmic organelle motors isolated from the nematode *C. elegans* (Lye et al., 1987) and from the giant amoeba *Reticulomyxa* (Euteneuer et al., 1988) showed a similar pattern of inhibitor sensitivity. HMW-2 therefore expresses the same pattern of pharmacologic susceptibility as other dynein-like cytoplasmic motors.

The Sertoli cell is a polar cell that actively secretes many proteins into the seminiferous tubular lumen (Rich and de Kretser, 1983). For example, transferrin is taken up at the basal Sertoli cell plasma membrane by receptor-mediated endocytosis (Morales and Clermont, 1986), iron is shuttled across the cell and subsequently secreted as testicular transferrin from the apical surface (Djakiew et al., 1986). Within the Sertoli cell cytoplasm, abundant membranous organelles are co-distributed with microtubules (Vogl et al., 1983*a*). Sertoli cell microtubules are crucial to the intracellular transport of smooth endoplasmic reticulum and likely play a role in translocation of germ cells within the seminiferous epithelium (Vogl et al., 1983*b*). Filamentous links have been observed ultrastructurally which connect nearby Sertoli cell microtubules and vesicles (Russell, 1977). HMW-2 may be the cytoplasmic microtubule motor responsible for one or more of these intracellular transport pathways.

This is the first in-depth study of high molecular weight MAPs in a mammalian nonneuronal tissue. We initiated this examination of the Sertoli cell cytoskeleton because of earlier qualitative morphological reports of a similarity in the microtubule organization of the axon and Sertoli cell processes (Fawcett, 1975; Vogl et al., 1983*a*,*b*). We have studied morphological, structural and functional properties of Sertoli cell microtubules and observed a regular microtubule distribution, an abundance of high molecular weight MAPs and the presence of a microtubule-activated cytoplasmic dynein, features characteristic of the neuronal cytoskeleton. The testis and the nervous system also share a susceptibility to a group of toxicants, including the acrylamides, β,β′-iminodipropionitrile, carbon disulfide, hexacarbons, and chronically administered organophosphate esters. The common biologic feature which renders the nervous system and the testis uniquely vulnerable to this toxic injury is unknown. In most instances, the proposed subcellular target for injury is the cytoskeleton (Boekelheide, 1988*b*; Genter et al., 1987; Gottfried et al., 1985; Miller and Spencer, 1985; Papasozomenos et al., 1981; Seifert and Casida, 1982). Indeed, an effect upon axonal transport is common to many of these toxic agents (Miller and Spencer, 1985; Reichert and Abou-Donia, 1980; Weiss and Gorio, 1982). At least with the hexacarbons, the target cell for injury in the testis is the Sertoli cell (Boekelheide, 1988*a*; Chapin et al., 1983). These results lay the groundwork for an investigation of the following hypothesis: some toxicants which selectively injure the testis and nervous system do so by disruption of a shared microtubule-related function.

The authors thank Zosia K. Rybkowski and Sarah T. Brace for their assistance with the electron microscopy and Dr. Richard B. Vallee for helpful discussions.

This work was supported by grant R01-OH02191 from the National Insti-

tute for Occupational Safety and Health of the Centers for Disease Control and the International Life Sciences Institute Research Foundation.

Received for publication 11 March 1988, and in revised form 8 July 1988.

References

Amlani, S., and A. W. Vogl. 1988. Changes in the distribution of microtubules and intermediate filaments in the mammalian Sertoli cells during spermatogenesis. *Anat. Rec.* 220:143–160.

Bloom, G. S., T. A. Schoenfeld, and R. B. Vallee. 1984. Widespread distribution of the major polypeptide component of MAP-1 (microtubule associated protein 1) in the nervous system. *J. Cell Biol.* 98:320–330.

Boekelheide, K. 1987. 2,5-Hexanedione alters microtubule assembly. II. Enhanced polymerization of crosslinked tubulin. *Toxicol. Appl. Pharmacol.* 88:383–396.

Boekelheide, K. 1988*a*. Rat testis during 2,5-hexanedione intoxication and recovery. I. Dose response and the reversibility of germ cell loss. *Toxicol. Appl. Pharmacol.* 92:18–27.

Boekelheide, K. 1988*b*. Rat testis during 2,5-hexanedione intoxication and recovery. II. Dynamics of pyrrole reactivity, tubulin content, and microtubule assembly. *Toxicol. Appl. Pharmacol.* 92:28–33.

Brady, S. T. 1985. A novel brain ATPase with properties expected for the fast axonal transport motor. *Nature (Lond.).* 317:73–75.

Chapin, R. E., K. T. Morgan, and J. S. Bus. 1983. The morphogenesis of testicular degeneration induced in rats by orally administered 2,5-hexanedione. *Exp. Mol. Pathol.* 38:149–169.

Chapin, R. E., J. L. Phelps, B. E. Miller, and T. J. B. Gray. 1987. Alkaline phosphatase histochemistry discriminates peritubular cells in primary rat testicular cell culture. *J. Androl.* 8:155–161.

Clermont, Y., and H. Morgentaler. 1955. Quantitative study of spermatogenesis in the hypophysectomized rat. *Endocrinology.* 57:369–382.

Clermont, Y., and B. Perey. 1957. Quantitative study of the cell population of the seminiferous tubules in immature rats. *Am. J. Anat.* 100:241–267.

Djakiew, D., M. A. Hadley, S. W. Byers, and M. Dym. 1986. Transferrin-mediated transcellular transport of ^{59}Fe across confluent epithelial sheets of Sertoli cells grown in bicameral cell culture chambers. *J. Androl.* 7:355–366.

Euteneuer, U., M. P. Koonce, K. K. Pfister, and M. Schliwa. 1988. An ATPase with properties expected for the organelle motor of the giant amoeba, *Reticulomyxa. Nature (Lond.).* 332:176–178.

Fawcett, D. W. 1975. Ultrastructure and function of the Sertoli cell. *In* Handbook of Physiology. Endocrinology: Male Reproductive System. D. W. Hamilton and R. O. Greep, editors. Williams & Wilkins. Baltimore, MD. Vol. 5, Sect. 7:21–55.

Forman, D. S., K. J. Brown, and M. E. Promersberger. 1983. Selective inhibition of retrograde axonal transport by erythro-9-[3-(2-hydroxynonyl)]adenine. *Brain Res.* 272:194–197.

Genter, M. B., G. Szakal-Quin, C. W. Anderson, D. C. Anthony, and D. G. Graham. 1987. Evidence that pyrrole formation is a pathogenetic step in γ-diketone neuropathy. *Toxicol. Appl. Pharmacol.* 87:351–362.

Gibbons, I. R., M. P. Cosson, J. A. Evans, B. H. Gibbons, B. Houck, K. H. Martinson, W. S. Sale, and W.-J. Y. Tang. 1978. Potent inhibition of dynein adenosinetriphosphatase and of the motility of cilia and sperm flagella by vanadate. *Proc. Natl. Acad. Sci. USA.* 75:2220–2224.

Gibson, W. 1981. Protease-facilitated transfer of high-molecular-weight proteins during electrotransfer to nitrocellulose. *Anal. Biochem.* 118:1–3.

Gottfried, M. R., D. G. Graham, M. Morgan, H. W. Casey, and J. S. Bus. 1985. The morphology of carbon disulfide neurotoxicity. *Neurotoxicol.* 6: 89–96.

Hirokawa, N., G. S. Bloom, and R. B. Vallee. 1985. Cytoskeletal architecture and immunocytochemical localization of microtubule-associated proteins in regions of axons associated with rapid axonal transort: the β,β′-iminodipropionitrile-intoxicated axon as a model system. *J. Cell Biol.* 101:227–239.

Izant, J. G., and J. R. McIntosh. 1980. Microtubule-associated proteins: A monoclonal antibody to MAP-2 binds to differentiated neurons. *Proc. Natl. Acad. Sci. USA.* 77:4741–4745.

Kim, H., L. I. Binder, and J. L. Rosenbaum. 1979. The periodic association of MAP_2 with brain microtubules in vitro. *J. Cell Biol.* 80:266–276.

King, S. M., and G. B. Witman. 1987. Structure of the α and β heavy chains of the outer arm dynein from *Chlamydomonas flagella. J. Biol. Chem.* 262: 17596–17604.

Kosik, K. S., L. K. Duffy, M. M. Dowling, C. Abraham, A. McCluskey, and D. J. Selkoe. 1984. Microtubule-associated protein 2: monoclonal antibodies demonstrate the selective incorporation of certain epitopes into Alzheimer neurofibrillary tangles. *Proc. Natl. Acad Sci. USA.* 81:7941–7945.

Laemmli, U. K. 1970. Cleavage of structural proteins during the assembly of the head of bacteriophage T4. *Nature (Lond.).* 227:680–685.

Leblond, C. P., and Y. Clermont. 1952. Definition of the stages of the cycle of the seminiferous epithelium in the rat. *Ann. N.Y. Acad. Sci.* 55:548–573.

Lewis, S. A., P. Sherline, and N. J. Cowan. 1986*a*. A cloned cDNA encoding MAP1 detects a single copy gene in mouse and a brain-abundant RNA whose level decreases during development. *J. Cell Biol.* 102:2106–2114.

Lewis, S. A., A. Villasante, P. Sherline, and N.J. Cowan. 1986*b*. Brain-specific expression of MAP2 detected using a cloned cDNA probe. *J. Cell Biol.* 102:2098–2105.

Lowry, O. H., N. J. Rosebrough, A. L. Farr, and R. J. Randall. 1951. Protein measurement with the Folin phenol reagent. *J. Biol. Chem.* 193:265–275.

Lye, R. J., M. E. Porter, J. M. Scholey, and J. R. McIntosh. 1987. Identification of a microtubule-based cytoplasmic motor in the nematode *C. elegans. Cell.* 51:309–318.

Merril, C. R., D. Goldman, S. A. Sedman, and M. H. Ebert. 1981. Ultrasensitive stain for proteins in polyacrylamide gels shows regional variation in cerebrospinal fluid proteins. *Science (Wash. DC).* 211:1437–1438.

Miller, M. S., and P. S. Spencer. 1985. The mechanisms of acrylamide axonopathy. *Annu. Rev. Pharmacol. Toxicol.* 25:643–666.

Morales, C., and Y. Clermont. 1986. Receptor-mediated endocytosis of transferrin by Sertoli cells of the rat. *Biol. Reprod.* 35:393–405.

Morton, D. B. 1976. Lysosomal enzymes in mammalian spermatozoa. *In* Lysosomes in Biology and Pathology. J. T. Dingle and R. T. Dean, editors. Elsevier/North Holland, Amsterdam. 203–255.

Murphy, D. B., and G. G. Borisy. 1975. Association of high-molecular-weight proteins with microtubules and their role in microtubule assembly *in vitro. Proc. Natl. Acad. Sci. USA.* 72:2696–2700.

Nelson, W. O. 1951. Mammalian spermatogenesis: effect of experimental cryptorchidism in the rat and non-descent of the testis in man. *Recent Prog. Horm. Res.* 6:29–62.

Olmsted, J. B. 1986. Microtubule-associated proteins. *Annu. Rev. Cell Biol.* 2:421–457.

Papasozomenos, S. C., L. Autilio-Gambetti, and P. Gambetti. 1981. Reorganization of axoplasmic organelles following β,β′-iminodipropionitrile administration. *J. Cell Biol.* 91:866–871.

Parysek, L. M., C. F. Asnes, and J. B. Olmsted. 1984*a*. MAP-4: Occurrence in mouse tissues. *J. Cell Biol.* 99:1309–1315.

Parysek, L. M., J. J. Wolosewick, and J. B. Olmsted. 1984*b*. MAP-4: A microtubule-associated protein specific for a subset of tissue microtubules. *J. Cell Biol.* 99:2287–2296.

Paschal, B. M., H. S. Shpetner, and R. B. Vallee. 1987. MAP-1C is a microtubule-activated ATPase which translocates microtubules *in vitro* and has dynein-like properties. *J. Cell Biol.* 105:1273–1282.

Paschal, B. M., and R. B. Vallee. 1987. Retrograde transport by the microtubule-associated protein MAP-1C. *Nature (Lond.).* 330:181–183.

Penningroth, S. M., A. Cheung, P. Bouchard, C. Gagnon, and C. W. Bardin. 1982. Dynein ATPase is inhibited selectively in vitro by *erythro*-9-[3-2-(hydroxynonyl)]adenine. *Biochem. Biophys. Res. Commun.* 104:234–240.

Reichert, B. L., and M. B. Abou-Donia. 1980. Inhibition of fast axoplasmic transport by delayed neurotoxic organophosphorus esters: a possible mode of action. *Mol. Pharmacol.* 17:56–60.

Rich, K. A., and D. M. de Kretser. 1983. Spermatogenesis and the Sertoli cell. *In* The Pituitary and Testis: Clinical and Experimental Studies. D. M. de Kretser, H. G. Burger, and B. Hudson, editors. Springer Verlag, Berlin. 84–105.

Russell, L. 1977. Observations on rat Sertoli ectoplasmic ("junctional") specializations in their association with germ cells of the rat testis. *Tissue Cell.* 9:475–498.

Russell, L. D., M. Tallon-Doran, J. E. Weber, V. Wong, and R. N. Peterson. 1983. Three-dimensional reconstruction of a rat stage V Sertoli cell: III. A study of specific cellular relationships. *Am. J. Anat.* 167:181–192.

Seifert, J., and J. E. Casida. 1982. Possible role of microtubules and associated proteases in organophosphorus ester-induced delayed neurotoxicity. *Biochem. Pharmacol.* 31:2065–2070.

Sloboda, R. D., W. L. Dentler, and J. L. Rosenbaum. 1976. Microtubule-associated proteins and the stimulation of tubulin assembly *in vitro. Biochemistry.* 15:4497–4505.

Sloboda, R. D., S. A. Rudolph, J. L. Rosenbaum, and P. Greengard. 1975. Cyclic AMP-dependent endogenous phosphorylation of a microtubule-associated protein. *Proc. Natl. Acad. Sci. USA.* 72:177–181.

Valdivia, M. M., J. Avila, J. Coll, C. Colaco, and I. V. Sandoval. 1982. Quantitation and characterization of the microtubule associated MAP_2 in porcine tissues and its isolation from porcine (PK15) and human (HeLa) cell lines. *Biochem. Biophys. Res. Commun.* 105:1241–1249.

Vale, R. D., J. M. Scholey, and M. P. Sheetz. 1986. Kinesin: possible biological roles for a new microtubule motor. *Trends Biochem. Sci.* 11:464–468.

Vallee, R. B. 1982. A taxol-dependent procedure for the isolation of microtubules and microtubule-associated proteins (MAPs). *J. Cell Biol.* 92:435–442.

Vallee, R. B. 1985. On the use of heat stability as a criterion for the identification of microtubule associated proteins (MAPs). *Biochem. Biophys. Res. Commun.* 133:128–133.

Vallee, R. B., and G. S. Bloom. 1984. High molecular weight microtubule-associated proteins (MAPs). *Mod. Cell Biol.* 3:21–75.

Vallee, R. B., and F. C. Luca. 1985. Light chain content and other criteria for the identification of microtubule associated protein 1A and microtubule associated protein 1B. *In* Microtubules and Microtubule Inhibitors. M. De Brabander and J. De Mey, editors. Elsevier/North Holland, Amsterdam. 129–144.

Vogl, A. W., Y. C. Lin, M. Dym, and D. W. Fawcett. 1983*a*. Sertoli cells of the golden-mantled ground squirrel (*Spermophilus lateralis*): a model system for the study of shape change. *Am. J. Anat.* 168:83–98.

Vogl, A. W., R. W. Linck, and M. Dym. 1983*b*. Colchicine-induced changes in the cytoskeleton of the golden-mantled ground squirrel (*Spermophilus lateralis*) Sertoli cells. *Am. J. Anat.* 168:99–108.

Weber, J. E., L. D. Russell, V. Wong, and R. N. Peterson. 1983. Three-dimensional reconstruction of a rat stage V Sertoli cell: II. Morphometry of Sertoli-Sertoli and Sertoli-germ-cell relationships. *Am. J. Anat.* 167:163–179.

Weiss, D. G., and A. Gorio. 1982. Axoplasmic transport in Physiology and pathology. Springer-Verlag, Berlin. 92–122.

Wiche, G., E. Briones, C. Koszka, U. Artlieb, and R. Krepler. 1984. Widespread occurrence of polypeptides related to neurotubule-associated proteins (MAP-1 and MAP-2) in non-neuronal cells and tissues. *EMBO (Eur. Mol. Biol. Organ.) J.* 3:991–998.

Wong, V., and L. D. Russell. 1983. Three-dimensional reconstruction of a rat stage V Sertoli cell: I. Methods, basic configuration, and dimensions. *Am. J. Anat.* 167:143–161.

Wuerker, R. B., and J. B. Kirkpatrick. 1972. Neuronal microtubules, neurofilaments and microfilaments. *Int. Rev. Cytol.* 33:45–75.